Atmospheric Environment 272 (2022) 118931

Contents lists available at ScienceDirect

Atmospheric Environment

journal homepage: www.elsevier.com/locate/atmosenv

Connection between lung deposited surface area (LDSA) and black carbon (BC) concentrations in road traffic and harbour environments

Teemu Lepistö [a,*], Heino Kuuluvainen [a], Henna Lintusaari [a], Niina Kuittinen [a], Laura Salo [a], Aku Helin [b], Jarkko V. Niemi [c], Hanna E. Manninen [c], Hilkka Timonen [b], Pasi Jalava [d], Sanna Saarikoski [b], Topi Rönkkö [a]

[a] Aerosol Physics Laboratory, Physics Unit, Tampere University, P.O. Box 692, 33014, Tampere, Finland
[b] Atmospheric Composition Research, Finnish Meteorological Institute, P.O. Box 503, Helsinki, 00101, Finland
[c] Helsinki Region Environmental Services Authority HSY, P.O. Box 100, 00066 HSY, Helsinki, Finland
[d] Inhalation Toxicology Laboratory, Department of Environmental and Biological Sciences, University of Eastern Finland, P.O. Box 1627, 70211, Kuopio, Finland

HIGHLIGHTS

- Characteristics of LDSA investigated in a harbour and near traffic in Helsinki area.
- BC emitted from marine traffic is linked to higher LDSA per mass than road traffic.
- BC emissions contribute more to LDSA (30–47% of total LDSA) than to PM_1 (7–14%).
- In the harbour, higher absorption Ångström exponent was connected to higher LDSA.
- Health hazard of BC might be related to high LDSA and other co-emitted species.

ARTICLE INFO

Keywords:
Urban environment
Traffic emissions
Particle size distribution
Marine traffic
Black carbon
LDSA

ABSTRACT

Black carbon (BC) is one of the main components of ambient particulate matter. Previous studies have suggested that BC is more toxic than $PM_{2.5}$ (mass concentration of all sub-2.5 μm particles). One possible reason for the greater toxicity is that BC is typically in a size range which penetrates easily into lung alveoli and BC particles have a large surface area due to their fractal structure. Due to these properties, toxic gaseous compounds can condensate on the surface of BC particles and then be transported effectively into human lungs, causing a large lung-depositing surface area (LDSA) of particles. In this study, we investigated the relationship between BC and LDSA concentrations in street canyon, highway, and harbour environments in the Helsinki Metropolitan area. In all the studied environments, BC and LDSA concentrations were strongly correlated. In the harbour, cases where marine traffic was considered as the main emission source, the average LDSA per BC mass was 2.4–2.7 times higher than in the road traffic environments. This result was linked to a larger lung depositing size of BC, suggesting that condensation and coagulation of other co-emitted compounds can have a major role in the lung deposition of BC. Thus, BC emissions from marine traffic can cause higher exposure of other co-emitted toxic compounds in the human lungs than the road traffic. The fraction of LDSA linked to BC emissions in the street canyon, the highway, and the harbour were 33%, 30%, and 47%, respectively, whereas the fractions of BC mass in PM_1 concentration were 14%, 14%, and 7%, respectively. The results show that BC emissions contribute much more to LDSA than to mass concentration, which indicates that the possible strong negative health effects linked to ambient BC mass concentration could be related to the high LDSA concentration.

1. Introduction

Ambient fine particles are known to cause major health related problems worldwide. It has been recently estimated that globally fine particulate matter ($PM_{2.5}$) emitted from fossil fuel combustion may have caused 8.7–10.2 million premature deaths annually during years

* Corresponding author. Korkeakoulunkatu 3, 33720, P.O.Box 692, 33014, Tampere, Finland.
E-mail address: teemu.lepisto@tuni.fi (T. Lepistö).

https://doi.org/10.1016/j.atmosenv.2021.118931
Received 24 September 2021; Received in revised form 13 December 2021; Accepted 30 December 2021
Available online 5 January 2022

2012–2018 (Vohra et al., 2021), which substantially exceeds 4.2 million in previous estimations (e.g. Cohen et al., 2017), where all sources of $PM_{2.5}$ were included. Furthermore, fine particles contribute to multiple severe diseases, including lung cancer, cardiopulmonary and neurological diseases (Pope et al., 2002; Raaschou-Nielsen et al., 2013; Power et al., 2016). The fine particle emissions are a major problem especially in urban environments as high pollution levels from various emissions sources are combined with the high population density.

Even though the evidence for negative health effects of fine particle pollution is indisputable, it is still unclear which properties of the particles are the main causes for these effects. Usually, the negative health effects are linked to the $PM_{2.5}$ mass concentration (Dockery et al., 1993; Burnett et al., 2014; Lelieveld et al., 2015). One reason for this is that the $PM_{2.5}$ concentrations are monitored widely around the world, which leads the epidemiological studies to focus on the mass concentration of particles. Also, current regulations regarding the particulate emissions are mostly based on the mass concentration of particles (Gemmer and Xiao, 2013). However, the correlation between premature deaths and the $PM_{2.5}$ concentration varies from place to place: Equal $PM_{2.5}$ concentration causes significantly less premature deaths in China than e.g. in Europe (Li et al., 2019). This observation emphasizes the need to understand which sources of fine particle emissions are more harmful than others, and which properties of fine particles are the most relevant. Thus, other metrics parallel to $PM_{2.5}$ are needed in the monitoring of fine particle levels in cities to understand the connection between fine particle pollution and the health effects.

One way to estimate the health risk caused by particles is to analyse the particle deposition in the human respiratory tract. Particle deposition efficiency in the human respiratory tract depends on the particle size (ICRP, 1994). Thus, by analysing the particle size distributions of the sample aerosol, it is possible to estimate the fraction of particles that ends up into different regions of the human respiratory tract. One metric, which utilizes this information about the particle deposition efficiencies, is the lung deposited surface area (LDSA) of particles. The LDSA is a metric that estimates the surface area concentration of particles that deposit in the alveolar region of the human lungs. The alveolar region may be the most crucial regarding the particle health effects since the interaction between respiration and pulmonary circulation takes place there. It has been found that particles in the blood circulation can end up even in the human brain (Heusinkveld et al., 2016). As mentioned, the LDSA estimates the alveolar deposition with the surface area concentration of particles. Studies have found that the surface area concentration of particles may have stronger correlation with the negative health effects than e.g. number or mass concentration (Brown et al., 2001, Oberdorster et al., 2005). Thus, the particle surface area must be explored as a relevant metric when it comes to understanding the deposition of particles into the human lungs. Furthermore, studies have shown that reduced lung function (Patel et al. 2018), subclinical atherosclerosis (Aguilera et al., 2016), and mortality (Hennig et al., 2018) are more strongly associated with the LDSA than with the $PM_{2.5}$ or PM_{10}. Also, the delivered dose of particle surface area has been found to be the most important metric for acute pulmonary inflammation with insoluble particles with mouses and rats (Schmid and Stoeger, 2016). These findings emphasize the importance of the LDSA as a metric when considering the health effects caused by the particle exposure.

One of the main components of ambient particulate matter is black carbon (BC) which is emitted from incomplete combustion processes. Black carbon particles are insoluble, refractory and they strongly absorb light at all visible wavelengths. Primary BC particles are agglomerated as they consist of small carbon spherules (Bond et al., 2013). During the exhaust dilution and cooling processes, the black carbon particles grow as initially gaseous exhaust compounds condensate on their surface and this growth continues in the atmosphere e.g. due to photochemical processing (Krasowsky et al., 2016) and coagulation. Thus, properties of ambient BC particles depend highly on the co-emitted species and the atmospheric conditions. When considering the particle number size distributions, ambient BC particles form a log-normal distributed soot mode, which is typically in the size range from 30 nm to 300 nm (Kumar et al., 2010). It has been observed that ambient BC is harmful for human health and negative health effects may be stronger than with the $PM_{2.5}$ concentration (Janssen et al., 2011).

One possible explanation for the stronger health effects of ambient BC could be its association with the LDSA. Various studies have reported similar trends between BC and LDSA concentrations (e.g. Jeong et al., 2017; Lin et al., 2022). BC emissions correlate with the LDSA concentrations of particles especially near traffic (Hama et al., 2017; Cheristanidis et al., 2020; Kuula et al., 2020), but also in residential areas where wood combustion causes high BC concentrations (Kuula et al., 2020). This association between BC and LDSA can be explained with the sizes of the ambient BC particles. In urban air, the peak of the LDSA size distribution of particles is typically near the size of 100 nm (Kuuluvainen et al., 2016), which corresponds to the typical sizes of the ambient BC particles. This connection suggests that BC particles can act as carriers of toxic gaseous compounds, which condensate on particle surfaces, into the alveolar region of the human respiratory tract. As mentioned, in mouse and rat studies, the delivered dose of particle surface area has shown to be the most relevant metric for pulmonary inflammation with insoluble particles, which indicates that LDSA is an important metric for the ability of insoluble BC particles to carry toxic materials into the lung alveoli. Thus, the atmospheric condensation may be a significant factor in the health effects caused by ambient BC as the toxic compounds can effectively be transported into the human lungs on BC particles.

Even though, the correlations between BC and LDSA have been analysed in previous studies (e.g. Reche et al., 2015; Hama et al., 2017; Cheristanidis et al., 2020; Kuula et al., 2020), the role of ambient BC in the lung-deposition of particles has not been investigated in-detail. First, it is unknown which fraction of LDSA is linked to the BC emissions. Second, it is not well-known how the transportation of other compounds on BC particles into human lungs depend on the environment. It is likely that the toxicity related to BC depends on the other co-emitted compounds and, therefore, on the emission source. Third, according to our knowledge, the characteristics and sizes of lung-depositing particles have been reported only from traffic sites (e.g. Salo et al., 2021) or residential areas (e.g. Pirjola et al., 2017) before. Also, the correlation between BC and LDSA has been studied mainly in traffic (Cheristanidis et al., 2020; Kuula et al., 2020), urban background (Reche et al., 2015, Hama et al., 2017) or residential area (Kuula et al., 2020) environments. It is probable that the lung deposition of particles and BC differ notably e.g. in harbours in comparison with the aforementioned environments as marine traffic is a significant source of e.g. SO_2, NO_x and volatile organic compounds (VOC) (Cesari et al., 2014; Xiao et al., 2018), which contribute to secondary aerosol formation and condensation (Gentner et al., 2017). Thus, it is important to analyse the characteristics of lung-depositing particles in various different environments to understand why the connection between the negative health effects and the $PM_{2.5}$ varies in different areas. Last, by understanding the role of BC in the particle lung deposition, it could be possible to explain, why BC seems more toxic than $PM_{2.5}$ when the particle mass is considered.

The objective of our study is to investigate the connection between BC and LDSA concentrations in detail in different urban environments. We report the fraction of LDSA linked to BC, which is important information for the estimation of health effects caused by ambient BC. The stationary and mobile measurements of the study were carried out in street canyon, highway and harbour environments in the Helsinki Metropolitan area, Finland. In these environments, the characteristics of the lung depositing particles were analysed with the LDSA size distribution. Additionally, we report the surface area of the non-volatile aerosol fraction and the absorption Ångström exponent values of the measured aerosol and investigate their association with both BC and LDSA. These metrics give valuable information of the primary BC particles and the effects of atmospheric aging processes and particle growth

on the LDSA. Furthermore, we report the average BC and LDSA concentrations in the studied environments. While traffic site concentrations of LDSA and BC have been reported previously, according to our knowledge, the characteristics of the lung depositing particles in harbour areas have not been analysed previously.

2. Experimental

2.1. Measurement locations

The ambient measurements of this study took place in the Helsinki Metropolitan area on August 13 - 23, 2019. The Helsinki Metropolitan area has a population of approximately 1.2 million. The measurements were done with Aerosol and Trace-gas mobile laboratory (ATMo-Lab by Tampere University), which was utilized in both stationary and driving measurements. The chosen urban environments for the stationary measurements were a street canyon, a highway, and a harbour. The driving measurement route included the locations of the stationary measurements. The stationary measurement locations and the driving route are shown in Fig. 1.

The street canyon measurement site was in the Helsinki central area (Mäkelänkatu 50) and is marked with a red circle in Fig. 1. The exact measurement location was on a kerbside next to an air quality monitoring supersite operated by Helsinki Region Environmental Services Authority (HSY). In 2019, an average of 28 000 vehicles drove pass the measurement station every weekday (Statistics of the City of Helsinki). The width of the street canyon is 42 m, and the adjacent buildings are 17 m tall. The buildings on both sides of the canyon and the trees in the middle of traffic lanes weaken the dilution processes of the pollutants, which is typical in street canyons (Karttunen et al., 2020). Thus, the measured aerosol can be considered as a mixture of fresh and aged exhaust from the traffic. The in-depth characterization of particulate matter at this street canyon site has been presented in Barreira et al. (2021).

The highway measurement location was next to Länsiväylä in Espoo (closest address Kuitinmäentie 31) and is marked with a blue circle in Fig. 1. The measurement location was next to HSY's air quality monitoring station, which is located on the Northern side of Länsiväylä highway, approximately 20 m from the road. On average, 70 000 vehicles passed the measurement station in Länsiväylä during weekdays in 2019. The average traffic rate in adjacent Kuitinmäentie (40 m North from the station) was 12 000 vehicles per weekday (Statistics of the City of Espoo). The measurement site was in an open environment, therefore, the emissions from the traffic dilute quickly, which emphasizes the differences in the aerosol aging processes in comparison with the street canyon measurement site.

The stationary measurements in the harbour area were done at two different locations. The main location (Harbour A) was in West Harbour next to a HSY's air quality monitoring station (Tyynenmerenkatu 8) and is marked with a purple circle in Fig. 1. The distance from the station to the closest ship was approximately 60 m. The station was next to a passenger traffic parking lot and 50 m away from Tyynenmerenkatu, which has an average traffic rate of 6000 vehicles on weekdays (Statistics of the City of Helsinki). Thus, the measured aerosol consists of emissions from both road and marine traffic. In Harbour A location, it was possible to compare the data from ATMo-Lab measurements with SO_2 concentration measured in the monitoring station. The other stationary location (Harbour B) was in Hernesaari (Munkkisaaren laituri), which is in the other side of the harbour area and is marked with a pink circle in Fig. 1. In this location, the measured aerosol can be considered

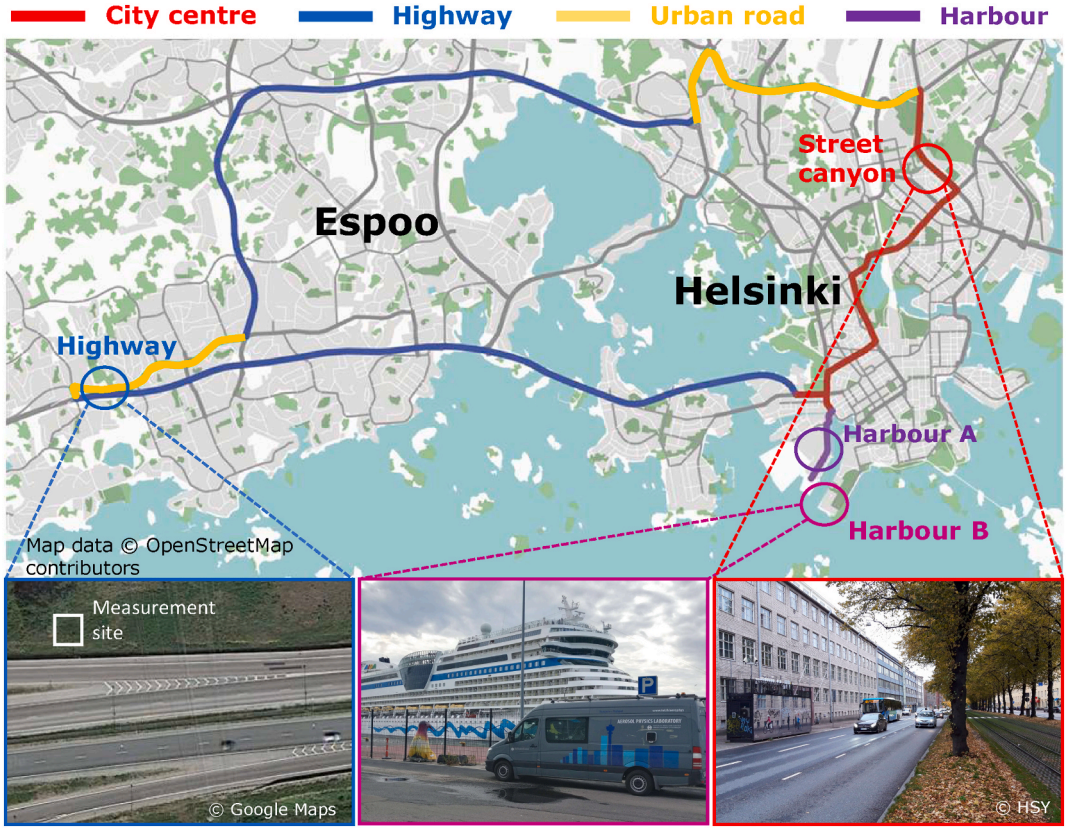

Fig. 1. Measurement locations on map. Stationary measurement locations are marked with circles. The driving measurement route was divided in four different sections which were city centre, highway, harbour and urban road. These sections are marked with red, blue, purple, and orange lines, respectively. Also, ATMo-Lab measurement van is shown in the harbour area picture. (For interpretation of the references to colour in this figure legend, the reader is referred to the Web version of this article.)

to consist mainly of the emissions from marine traffic since the location was relatively far away from other emissions sources. In Harbour B, the nearest road with regular vehicular traffic was approximately 600 m away and the passenger loading point on the other side of the harbour was approximately 250 m away. However, during the measurements, wind was directly from the sea (South-West), thus it is unlikely that the vehicular traffic has affected the measurements in Harbour B. The measurement times in Harbour B location were limited as there was no electricity supply for ATMo-Lab. During the measurement days in the harbour, 26–28 ships arrived or departed during the day. In the harbour measurements, 91% of the time was measured in Harbour A and 9% in Harbour B location.

In addition to the stationary measurements, driving measurements were carried out in the measurement route shown in Fig. 1. The route was divided to four different environments: city centre (marked with red), highway (blue), harbour area (purple), and urban road (orange). The area classified as city centre had typical features of central areas such as street canyons, traffic jams, and considerable number of pedestrians. Roads classified as highway had speed limits of 80–100 km/h and at least four lanes in total. The harbour area included roads that were in West Harbour. The urban road included areas which did not fit in the definitions of the other three environments but were still highly influenced by the nearby city activity. The driving measurements were conducted to ensure that the stationary measurement locations are representative of the environments they were categorized to represent.

The measurements were performed during 9 working days. The measurements were carried out in one location per day to achieve long time series data. Measurements took place between 6 and 22 and there were two measurement days in each stationary measurement location. For example, the stationary measurements in street canyon took place on August 13th and 20th. In addition, three days were reserved for driving measurement only. The durations of the measurements and the main measurement locations during the measurement days are summarized in the Supplementary (Tables S1 and S2). Weather and background concentration data are also provided in the Supplementary (Table S1 and Figs. S1 and S2). The average temperature and relative humidity of the measurement days varied from 16.4 °C to 18.5 °C and from 56.3% to 89.8%, respectively. The wind conditions were stable, and the wind was mainly from the South-West during the campaign. During the measurement weeks, there were not clear episodes of regionally or long range transported particles, since the background concentration levels of LDSA and BC were low and stable (Supplementary Fig. S2). More detailed maps of the stationary measurement locations are provided in Supplementary (Figs. S3–S5).

2.2. Measurement setup and instruments

The measurements were conducted with ATMo-Lab measurement van (shown in Fig. 1). The sample inlet was above the van's wind shield at a height of 2.2 m. The sample was then divided for the instruments which were in the back end of the van. The exhaust pipe of the measurement van is located in the rear-end of the van. Therefore, the risk of self-sampling with ATMo-Lab can be considered to be minimal during the driving measurements.

The number size distributions of ambient and non-volatile particles were measured simultaneously with two Electrical Low-Pressure Impactor ELPI+ (Dekati Ltd.) units. ELPI + charges the sample aerosol in a unipolar diffusion charger and then classifies the particles according to their aerodynamic diameter in a cascade impactor. The size distributions of particles can then be calculated by measuring the electrical current caused by the particles in the impactor stages with 1 s time resolution. ELPI + has 14 impactor stages in a size range from 6 nm to 10 μm. The operation principle of ELPI is described in detail in Keskinen et al. (1992) and Marjamäki et al. (2000). The calibration of the renewed ELPI+ is presented in Järvinen et al. (2014). In addition to the number size distributions, ELPI+ was used to measure the LDSA concentrations and size distributions. Furthermore, the surface area concentrations and PM_1 concentrations of particles were determined from ELPI + by integrating the measured particle number size distributions.

The size-segregated measurement data of ELPI + enables measurement of LDSA concentration and size distributions. As mentioned in the introduction, the lung deposition efficiency of particles depends significantly on the particle size. Therefore, stage-specific conversion factors from electric current data of ELPI + impactor stages to LDSA concentration can be determined by utilizing the particle lung deposition efficiency functions and the particle size information of the impactor stages (Lepistö et al., 2020). The stage-specific conversion factors enable measurement of the LDSA concentration and size distribution with the whole ELPI + size range.

BC mass concentration was measured with AE33 Aethalometer (Magee Scientific). The operation principle of an aethalometer is described in detail in Drinovec et al. (2015). Shortly, AE33 determines the BC mass concentration by measuring the attenuation caused by particles collected onto a filter tape. AE33 measures the attenuation at seven different wavelengths of light. By measuring the attenuation, AE33 determines the aerosol light absorption coefficients ($b_{abs}(\lambda)$), which is then converted to equivalent BC (eBC) mass concentrations by dividing the determined $b_{abs}(\lambda)$ values with the mass absorption cross-section (MAC(λ)). Usually, also in this study, the data from the wavelength of 880 nm is used in the determination of the BC concentration. The data from other wavelengths can be used for source appointment analysis and for determining the absorption Ångström exponent of the measured aerosol (Sandradewi et al., 2008). The absorption Ångström exponent describes the spectral dependence of light absorption. The absorption Ångström exponent depends on the fuel combusted (Kirchstetter et al., 2004) but it is also affected by the primary particle size and particle coating, e.g. thickness and chemical composition (Lack and Cappa, 2010; Helin et al., 2021; Virkkula et al., 2021). Therefore, the absorption Ångström exponent can be used to characterize particles with different chemical composition and emission sources. For road traffic influenced aerosol, the absorption Ångström exponent is typically near 1 (Kirchstetter et al., 2004; Zotter et al., 2017; Helin et al., 2018). With AE33, the absorption Ångström exponent (α) can be determined by the formula

$$\alpha = -\frac{\ln b_{abs}(470\ nm)/b_{abs}(950\ nm)}{\ln \frac{470\ nm}{950\ nm}} \quad (1)$$

In this study, a cyclone was used to cut the upper limit of AE33 detection size range to 1 μm.

A thermodenuder was used in the measurement of the non-volatile particles. In the thermodenuder, the sample aerosol is heated causing evaporation of the volatile compounds of the aerosol. After the evaporation, the sample is cooled down and the evaporated compounds are absorbed into active charcoal due to the thermophoretic forces. Therefore, after the thermodenuder, only the non-volatile particles are left in the sample aerosol. In this study, the sample aerosol was heated to 265 °C temperature. The thermodenuder model used in this study is the same as in Heikkilä et al. (2009) and Amanatidis et al. (2018). The estimated particle losses with the thermodenuder were corrected in the data based on the loss measurements presented in Heikkilä et al., (2009).

2.3. Data processing

During the measurements, all the instruments logged measurement data with 1 s time resolution. However, data from the stationary measurements has been analysed with 1 min resolution to reduce the noise in AE33 data. This resolution change was done by calculating the arithmetic minute average of the measurement data. In the driving measurements, the measurement data was averaged to 30 s resolution, because the averaging period of 1 min was too long for the shorter parts in the driving route.

The measurement results presented in this article are calculated with the geometric mean of the measured concentrations. The incidence of the measured concentrations in this study were log-normally distributed, therefore the geometric mean gives more representative results of the most common situation in the environment than the arithmetic mean. In this study, the particle effective density is assumed to be the unit density of 1 g/cm^3. This assumption is needed as ELPI + size classification is based on the aerodynamic diameter of particles. Therefore, the effective density of the measured particles affects the measured concentrations e.g. PM_1 and LDSA. However, the unit density approximation with ELPI + LDSA measurement is known to be relatively accurate when the effective density is known to be close to the unit density (Lepistö et al., 2020). For example, in a street canyon, the average effective density of particles with the mobility diameter of 100 nm are 0.66–0.70 and 1.30–1.38 with locally emitted and long-range transported aerosol, respectively (Rissler et al., 2014). The urban air aerosol is a mixture of locally emitted and background aerosol. Thus, the unit density approximation is reasonable. Also, it is assumed that the particles do not grow due to hygroscopicity in the human lungs, which is a common approximation in ambient LDSA measurements due to the measurement techniques. Primary BC particles are mainly hydrophobic (Henning et al., 2012; Happonen et al., 2013), but the hygroscopicity of BC particles can increase due to the atmospheric condensation processes and, therefore, increase the exposure of coated accumulation mode BC particles in the human lungs (Ching et al., 2020). Thus, it is possible that the connections between BC and LDSA might be slightly underestimated in the results. On the other hand, contribution of hygroscopic ultrafine particles could be overestimated in the measured LDSA concentration, which emphasizes the role of hydrophobic BC in the particle lung-deposition. The upper limit of the measurement size range in this study was 1 μm, which was chosen to minimize the effects of inertial particle losses in the sampling lines in the measurement results.

In section 3.5, the fraction of the total LDSA linked to the BC emissions in the studied environments is analysed by investigating the incidence of the measured LDSA per BC concentration -ratios. This was done to determine the most probable scenario in each studied environment. As the incidences (Fig. 7) were log-normally distributed, the most probable ratio and the deviations were determined by applying a log-normal fit in the measured probability distributions. In this calculation, cases with BC concentration lower than 0.5 μg/m^3 were ignored to reduce errors caused by very low BC concentration. Also, the background LDSA concentration, which was estimated not to depend on BC emissions from local sources, was deducted before the comparison of BC and LDSA concentrations. This background concentration was determined by calculating the average LDSA concentration during the low BC concentration (<0.5 μg/m^3) occasions. After this analysis, the determined most probable LDSA per BC ratios were applied in the calculation of the fraction of LDSA linked to BC emissions. The LDSA concentration linked to BC emission was determined by multiplying the measured BC concentration with the most probable LDSA per BC ratio in each studied environment. Then, the fraction of LDSA contributed by BC emissions was determined by comparing the calculated LDSA concentration linked to BC with the total measured LDSA concentration. With this calculation method, the effects of other co-emitted species (e.g. condensation and coagulation) on the lung-deposition of BC can be included in the analysis as well.

3. Results and discussion

3.1. Diurnal variation of BC and LDSA in the stationary measurements

The average LDSA and BC concentrations in the stationary measurement locations during different times of the day are shown in Table 1. The highest LDSA and BC concentrations were in the street canyon where the concentrations were the highest during morning rush hours from 6 to 9. Similar behaviour can be seen in the highway location. However, the average concentrations in the highway are notably lower than in the street canyon, which emphasizes the effects of the street canyon's surrounding buildings in the exhaust dilution processes. In the harbour, the highest concentrations were measured during afternoon from hours 15 to 18, whereas the concentrations were the lowest during the morning rush hours. The number of arriving or departing ships was also at the highest during afternoon and approximately 25% of the harbour activity occurred during hours from 15 to 18 (Supplementary, Table S3). The daily averaged BC concentrations are similar in the harbour and the highway, but the average LDSA is significantly higher in the harbour. These differences indicate that there is another main contributor in LDSA and BC concentrations in the harbour area than the road traffic, e.g. marine traffic. During afternoon and evening hours, the LDSA concentrations in the harbour area are similar to those in the street canyon, which suggests that the marine traffic can cause significant LDSA concentrations in harbour residential areas.

Table 1
The average LDSA and BC concentrations in the stationary measurement locations during different times of the day. Also, the 25th and 75th percentiles of the measured concentrations are shown.

	Street canyon		Highway		Harbour	
Time of the day	LDSA (μm^2/cm^3)	BC (μg/m^3)	LDSA (μm^2/cm^3)	BC (μg/m^3)	LDSA (μm^2/cm^3)	BC (μg/m^3)
6–9	*37.2 (26.7-48.4)*	*1.93 (1.08-3.01)*	*19.4 (15.5-24.8)*	*0.91 (0.61-1.45)*	*13.3 (9.0-16.6)*	*0.44 (0.22-0.75)*
9–12	*31.5 (22.6-39.8)*	*1.43 (0.94-1.95)*	*11.7 (10.1-14.0)*	*0.47 (0.32-0.77)*	*22.0 (14.5-28.8)*	*0.60 (0.41-0.91)*
12 - 15	*30.5 (21.1-40.3)*	*1.31 (0.78-1.98)*	*10.0 (8.4-11.4)*	*0.35 (0.24-0.55)*	*21.3 (14.5-24.0)*	*0.59 (0.37-0.89)*
15–18	*25.7 (18.8-30.3)*	*1.20 (0.75-1.77)*	*14.2 (11.5-17.2)*	*0.62 (0.48-0.75)*	*26.1 (19.6-30.2)*	*0.75 (0.55-1.11)*
18–22	*18.7 (15.0-21.3)*	*0.64 (0.36-1.01)*	*13.9 (10.9-16.8)*	*0.47 (0.37-0.59)*	*21.3 (17.9-23.1)*	*0.58 (0.43-0.72)*
Average 6–22	*27.2 (19.1-35.1)*	*1.17 (0.71-1.87)*	*13.6 (10.3-17.2)*	*0.54 (0.37-0.81)*	*20.3 (14.0-26.9)*	*0.59 (0.38-0.91)*

The LDSA and BC concentrations measured in this study are notably lower than in studies conducted in other cities. In the street canyon, both BC and LDSA concentrations are close to the urban background levels 1.34–2.33 μg/m^3 (Becerril-Valle et al., 2017 (Spain); Singh et al., 2018 (UK)) and 23–53 μm^2/cm^3 (Ntziachristos et al., 2007 (Los Angeles); Reche et al., 2015 (Barcelona); Hama et al., 2017 (Leicester)) reported in previous studies. In the harbour and the highway, the measured concentrations are mainly below these background levels. However, the BC and LDSA concentrations in road traffic environments are similar in comparison with the previous studies conducted in Helsinki area: Kuula et al. (2020) reported annual mean LDSA concentrations of 22 μm^2/cm^3 in traffic sites and 9.4 μm^2/cm^3 in an urban background site and Luoma et al. (2021) reported annual mean BC concentrations of 0.4–0.6 μg/m^3 in urban background sites and 0.7–1.0 μg/m^3 in traffic sites. In general, previous studies have found a decreasing trend for BC at a rate of 0.09–0.14 μg/m^3 per year at the Mäkelänkatu street canyon site (Barreira et al., 2021; Luoma et al., 2021).

The diurnal variation of the LDSA size distributions in the measurement locations is shown in Fig. 2. In the street canyon and the highway, the LDSA size distributions peak near the size of 100 nm, which agrees with the results from the previous studies conducted in traffic environments (Kuuluvainen et al., 2016; Pirjola et al., 2017). However, in the harbour area, particles in the size range 200–400 nm dominate the LDSA size distribution. Thus, the sizes of lung depositing

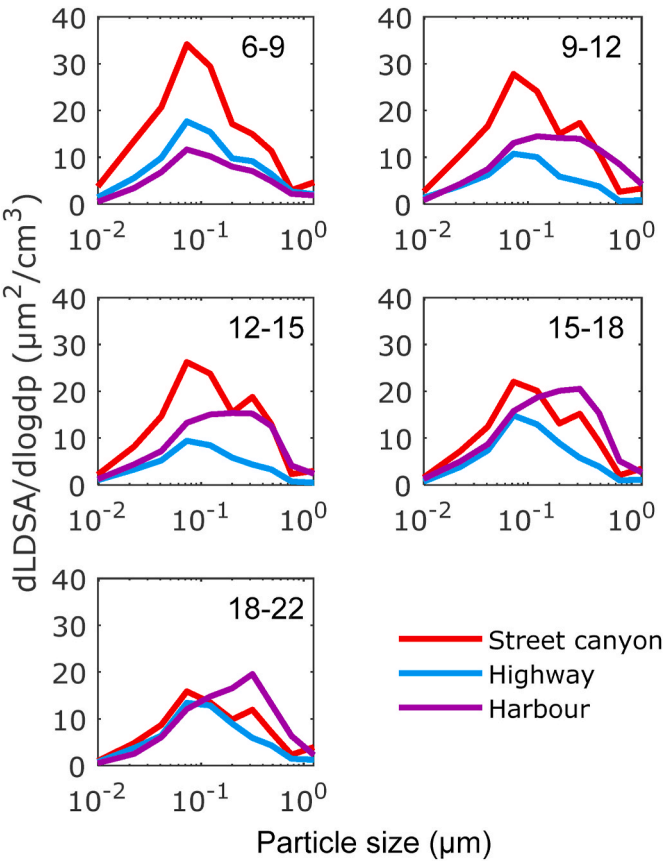

Fig. 2. Average LDSA size distributions in the stationary measurement locations during different times of the day.

particles are notably larger in the harbour than in the road traffic environments, which indicate that the marine traffic can cause higher LDSA per particle number than the road traffic. Also, the sizes of lung depositing particles increase during the day in the harbour. Typically, the larger particle size is an indication of aged aerosol as, in the atmosphere, particles grow due to condensation and coagulation. Therefore, it is possible that the atmospheric aging processes can have a significant effect on the total LDSA in harbour areas. It is known that emissions from marine traffic include e.g. SO_2, NO_x and volatile organic compounds (VOC) (Cesari et al., 2014; Xiao et al., 2018), which contribute to secondary aerosol formation (Gentner et al., 2017). Also, it has been estimated that 60–70% of $PM_{2.5}$ emissions from marine traffic are linked to the secondary aerosol (Viana et al., 2014). It was observed that also the mean size of the non-volatile particles was larger in the harbour (geometric mean diameters (GMD) of particle surface area size distributions 133–207 nm) than in the road traffic environments (GMDs 99–141 nm, see the diurnal variation of the non-volatile particle size distributions in Supplementary Fig. S6). This result can be explained e.g. with the condensed organics and sulphates originated from marine engines as it has been found that the volatility of these compounds can be low (Ntziachristos et al., 2016).

The possible effects of the atmospheric aging processes can be seen in the street canyon as well since the LDSA size distribution has another mode near the size of 300 nm. This mode can be observed especially during afternoon and evening, which indicates the contribution of aged aerosol. Also, this mode near the size of 300 nm cannot be observed with the non-volatile particle surface area size distributions (Supplementary Fig. S6). Therefore, the aged aerosol can affect the total LDSA exposure notably in street canyons. This same behaviour cannot be seen in the highway, which suggest that an open environment can significantly reduce the total LDSA caused by the road traffic as the effects of the atmospheric aging processes are notably lower. In all, the differences in the LDSA size distributions between the studied environments show that the characteristics and properties of the lung-depositing particles are different in these environments, which suggests that it is likely that the health effects relating the particle exposure in these locations are also different.

The major contribution of particles larger than 300 nm in the LDSA in the harbour and the street canyon is an important observation when considering the detection efficiency of diffusion charger based LDSA sensors. Typically, these sensors determine the LDSA concentration by measuring the electric current caused by the diffusion charged sample aerosol and then converting this current to LDSA concentration by using more-or-less a single conversion factor. This method is reasonably accurate with particles smaller than 300–400 nm but with larger particles the detection efficiency drops rapidly (Todea et al., 2015; Lepistö et al., 2020). This upper limit of 300–400 nm is usually enough as in road traffic environments the LDSA peaks near the size of 100 nm. However, the size distributions in Fig. 2 suggest that in street canyon and harbour environments the diffusion charger based LDSA sensors could occasionally underestimate the measured concentrations. To consider the issue, the performance of the LDSA sensors was demonstrated with the single-factor LDSA calibration of ELPI+ (Lepistö et al., 2020) and compared to the stage-specific calibration used in this study. With this analysis, underestimation of over 10% in the LDSA concentration occurs in 15%, 11% and 31% of all measured concentrations in street canyon, highway and harbour, respectively. However, the error is mainly below 25% in all environments. This analysis is presented in-detail in Supplementary (Figs. S9–S11). In all, it is recommended to consider the typical particle size distributions in the measurement environments when monitoring the LDSA concentration with diffusion charger-based sensors that are calibrated to monitor the air quality in road traffic environments as the sensors might not always be reliable in other environments, such as harbours, or during times when aged particles dominate.

3.2. *Influence of BC on LDSA concentrations*

In Fig. 2, the mean size of the LDSA size distributions varied in the size range of 100 nm–400 nm, which indicates major contribution by ambient BC as the soot mode of BC particles is usually in the same particle size range (Kumar er al. 2010). To investigate the influence of BC emissions on LDSA in more detail, the correlation between BC and LDSA concentrations in the measurement locations were analysed. The effect of BC is investigated on both LDSA concentrations and size distributions and this analysis is shown in Fig. 3.

In Fig. 3, the increased BC concentrations clearly affect the LDSA in all the studied environments. In the street canyon and the highway, the linear regression fits between BC and LDSA concentrations are similar, which can be explained with the same emissions source i.e. road traffic. In the harbour, the scatter plot between BC and LDSA divides into two distinct trends with different slopes: The connection between BC and LDSA depends significantly on the absorption Ångström exponent (α) of the measured aerosol. Previous emission and ambient measurement studies have observed that high α values (e.g. from 1.2 to 2.5) can be associated with ship emissions (Corbin et al., 2018; Yu et al., 2018) whereas α values for road traffic influenced aerosol are typically below 1.20 (Kirchstetter et al., 2004; Zotter et al., 2017; Helin et al., 2018). In our study, in cases where α was greater than 1.20, the average LDSA concentration per BC mass was approximately 2.3 times higher than in cases where α was lower than 1.20. In cases, where α was lower than 1.20 the slope of the linear fit between BC and LDSA is similar in comparison with the road traffic environments. Similar dependency of α was not found in the street canyon and the highway (Supplementary Fig. S7). This observation supports the idea that the emissions from marine traffic could be recognized from their higher absorption Ångström exponent. Also, it was observed that both BC and LDSA concentrations in harbour

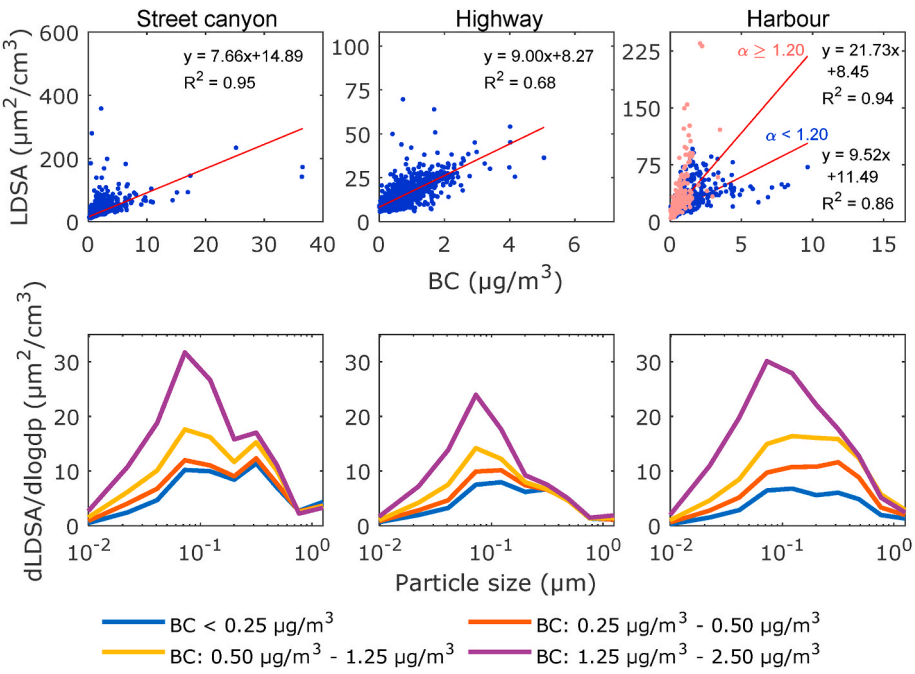

Fig. 3. The top row shows the correlation plots for LDSA and BC in the different stationary measurement locations along with linear regression fit lines. In the harbour area, separate fits are included for datapoints during which the Ångström exponent was above and below 1.20. The bottom row shows how increasing BC concentration affects the LDSA size distributions in each environment. Different BC concentration thresholds are marked with separated lines.

were linked to SO_2 concentration, and the group with higher α was recognisable from higher SO_2 per BC concentration -ratios as well (Supplementary, Figs. S12–13). Thus, the group with higher α can be considered as aerosol dominated by the marine traffic emissions. The result suggests that equal BC mass emitted from marine traffic can contribute to much higher LDSA than the road traffic. Possible reasons for this could be the atmospheric aging processes e.g. condensation and coagulation. However, the harbour area scatter plot indicates that the road traffic, e.g. ship loading and passenger traffic, is also a significant source of BC in harbour areas as the momentary BC concentrations can be high during the cases where α is lower than 1.20. It needs to be noted that the group of observations with α greater than 1.20 was measured in both harbour measurement locations. The separated scatter plot based on the harbour measurement location is shown in Supplementary (Fig. S14).

As can be seen in Fig. 3, the influence of increasing BC concentration on the LDSA size distributions differs notably between the harbour and road traffic environments as well. In the harbour, the effect of BC emissions can be seen in the size range from 50 nm to 500 nm whereas in the street canyon and in the highway the LDSA size distribution peaks in the size range from 50 nm to 200 nm as the BC concentration increases. As mentioned, marine traffic contributed to the measured concentrations in the harbour measurements, thus, it is justifiable to consider that the differences in the size distributions between the environments are related to the marine traffic emissions. The difference in the lung depositing sizes of BC particles between the environments indicate that composition of BC particles is also different, which supports the idea that the condensation of gaseous compounds and coagulation can have a crucial role in the lung deposition of black carbon in the harbour. Thus, the other co-emitted emission compounds may notably affect the toxicity of BC in harbour areas. However, also in the street canyon, increasing BC concentration affects the LDSA size distribution near the size of 300 nm. This observation suggests that the atmospheric aging processes can affect the lung deposition of BC notably in street canyons as well even though the effect is less significant than in the harbour. The difference between the street canyon and the highway area results indicates that the weakened emission dilution processes in the street canyon can explain this observation. However, it needs to be noted that the peak near the size of 300 nm can also be seen in the street canyon when the BC concentration is low, which is likely due to the background aerosol.

The surface area size distributions of the non-volatile particles, separated into four groups based on the similar BC concentration thresholds, are shown in Fig. 4. In the street canyon and the highway, the peaks of the distributions are near the size of 100 nm, which correspond well with the LDSA size distributions in these environments. In the harbour, the mean size of the size distributions is near the size of 150 nm, which is notably larger than in the road traffic environments. Therefore, also the sizes of the non-volatile particles linked to BC emissions are larger in the harbour than in the road traffic environments, which can be considered to be linked with the marine traffic emissions. This result can partly explain why BC emissions are linked to LDSA in larger particle sizes in the harbour. The results suggest that the primary BC particles from marine traffic emissions can be larger than from the road traffic. As mentioned earlier, the volatility of condensed compounds emitted from marine engines can be low (Ntziachristos et al., 2016), which could also explain the larger particle size of the non-volatiles linked to BC in the harbour. In all the studied environments, the correlation between BC and the non-volatile particle surface area was very strong (Supplementary Fig. S15), which indicates that the differences between the environments shown in Fig. 4 are mainly related to the black carbon emissions. However, it was noticed that, in the harbour, the non-volatile particle surface area concentration was occasionally high during low BC concentrations, which shows that the marine traffic is also a major source of other non-volatile particles than BC, e.g. metallic ash (Ntziachristos et al., 2016). In all, comparison between the size distributions in Figs. 3 and 4 show that the characteristics and features of the lung depositing BC particles differ notably in the road traffic and harbour environments, which is due to the differences between vehicular and marine traffic emissions. Thus, it is likely that also the health effects relating to the BC emissions are different in traffic and harbour environments.

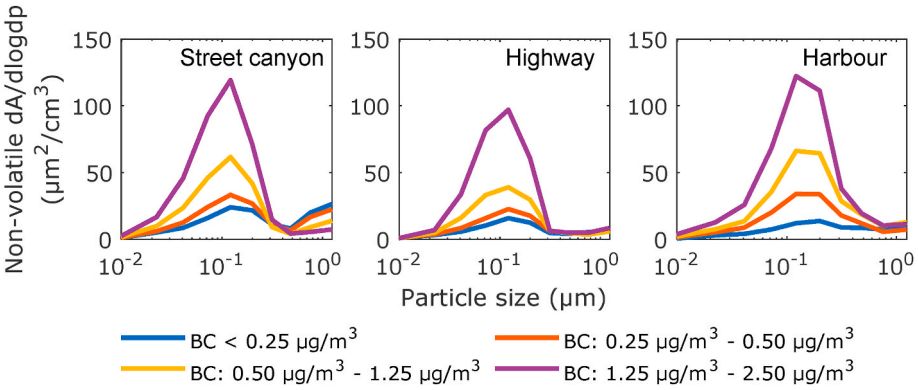

Fig. 4. The connection between the non-volatile particle surface area size distributions and the increasing BC concentration in the stationary measurements. Different BC concentration thresholds are marked with separate lines.

3.3. Harbour area

As seen in Fig. 3, the measurement results in the harbour can be divided into two distinct groups based on the absorption Ångström exponent (α) of the measured aerosol. The comparison between harbour area and the road traffic environments indicated that the aerosol with higher α was linked to the marine traffic emissions. To ensure that the higher α is indeed linked to the marine traffic, the average absorption Ångström exponents in the stationary measurement locations were calculated and shown in Table 2. As mentioned, Harbour B was located relatively far away from other emissions sources besides marine traffic. Thus, the data from Harbour B location can be considered to represent the emissions from the marine traffic. Now, in Harbour B, the average α of the measured aerosol is higher (1.32) than in the other environments (1.15–1.18), which indicates that, in the harbour measurement, the marine traffic emissions are linked to having higher absorption Ångström exponent values of the measured aerosol. This result is also supported by literature studies observing relatively high α values for aerosols originating from ship emissions (Corbin et al., 2018; Yu et al., 2018). It should be noted, that since our sampling site was located far away from residential wood combustion sources and since the temperature was warm during the campaign, it is not expected that the observed high α values are associated with wood combustion. In addition, the wind direction was mostly from the Baltic Sea, which unambiguously overrules wood combustion as a source for the observed α values.

An example timeseries data plot from Harbour B is shown in Fig. 5. The data was measured when a ship arrived in the harbour area. The plume from the ship caused clear spikes in LDSA, BC and non-volatile particle surface area concentrations. At other times, the measured concentrations were very low, which emphasizes the effects of marine traffic emissions in Harbour B location. More detailed results from Harbour B are shown in Supplementary (Figs. S16–S18, Table S4).

In Fig. 6, the average harbour area LDSA and non-volatile particle surface area size distributions during the cases with high and low α are compared with a normalized BC concentration. Cases where BC concentration was less than 0.5 μg/m^3 are not included in Fig. 6 as the normalization of low BC concentrations can cause uncertainties in the results. As can be seen, the LDSA size distribution is clearly affected by the higher α, which agrees with the results shown in Fig. 3. Also, the surface area concentration of the non-volatile particles increases significantly with the higher α. In both size distributions, the effect of higher α can be seen in the particle size range from 100 nm to 400 nm, which corresponds well with the sizes of the BC particles. Therefore, the differences in the size distributions are likely linked to the BC emissions. As mentioned earlier, the volatility of the condensed compounds from marine engines can be low (Ntziachristos et al., 2016), which could explain why equal BC mass contributes to higher non-volatile surface area when α is higher than 1.20. Also, the other primary particles emitted from marine engines can affect this result: Coagulation between

Table 2
The average absorption Ångström exponent in the stationary measurement locations. Also, the 25th and 75th percentiles are shown.

	Street canyon	Highway	Harbour A	Harbour B
Ångström exponent (α)	1.18 (1.13–1.23)	1.15 (1.07–1.22)	1.16 (1.06–1.27)	1.32 (1.14–1.43)

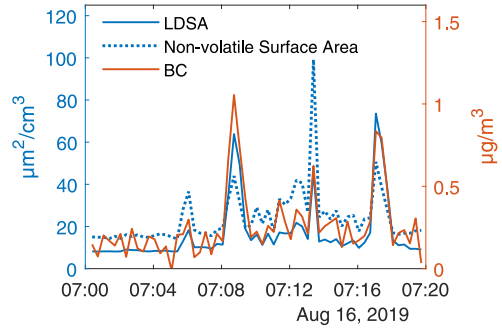

Fig. 5. Timeseries data from Harbour B location when a ship arrived the harbour area. Averaging period is 20s.

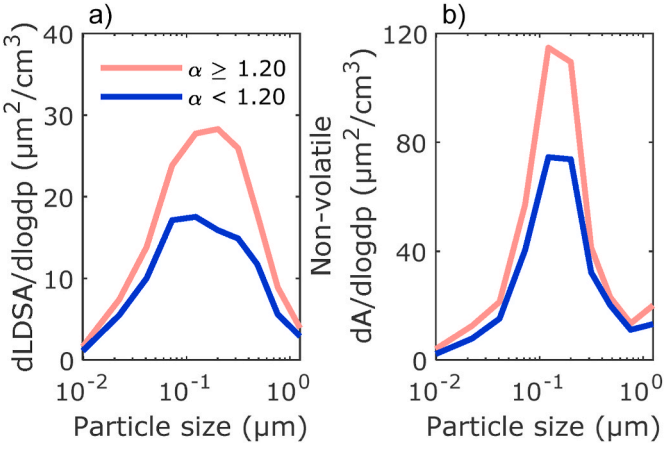

Fig. 6. LDSA (a) and non-volatile particle surface area (b) size distributions normalized with BC concentration in the harbour area stationary measurements when the Ångström exponent was above and below 1.20.

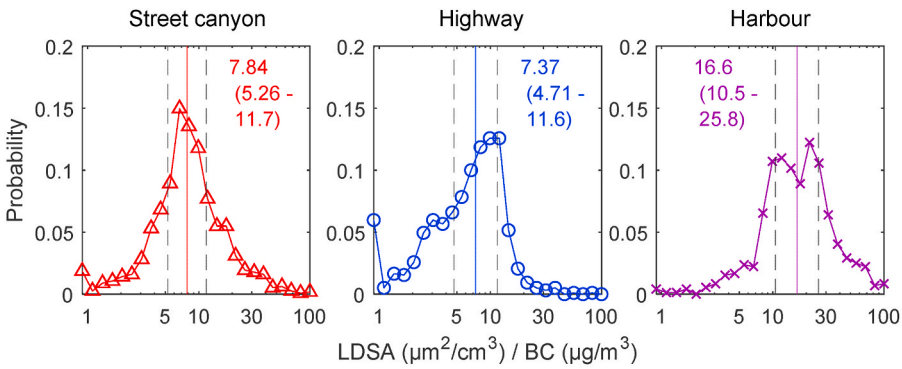

Fig. 7. Probability distributions of the measured LDSA per BC -ratios in the stationary measurement locations. Also, the most probable ratio and the 25th and the 75th percentiles are shown.

BC and other primary particles might explain why the difference relating to higher α is seen in the typical sizes of BC particles. In all, these observations indicate that the co-emitted compounds from marine traffic can significantly affect the lung deposition and the properties of BC particles. Thus, the toxicity of BC can be different in harbour areas than in road traffic environments. Also, the difference in α indicates that the chemistry of the lung depositing particles linked to marine traffic is different, which could mean different health effects. Thus, equal BC mass concentration may be related to more health-related problems in harbour areas than in road traffic environments as it is linked to higher LDSA and the chemical properties of the lung depositing particles are different.

However, as seen in Fig. 6, the mean size of both LDSA and non-volatile particle surface area size distributions during lower α values are still larger than in the road traffic environments. Therefore, it is possible that marine traffic has occasionally contributed to the measured aerosol when α has been lower than 1.20 due to concurrent road traffic emissions. Also, it needs to be noted that the value of the absorption Ångström exponent depends on the ship and the fuel type. For example, in engine laboratory measurements, it has been found that α with different marine fuels can be close to 1.0 (Helin et al., 2021). It is likely that the connection between BC and LDSA depends also notably on the ship and the fuel type. Therefore, different ships can cause significantly higher LDSA concentrations in harbour areas than others which emphasizes the importance of ship emission regulations.

3.4. Driving measurements

The results from the driving measurements are collected in Table 3. In the city centre, the average BC and LDSA concentrations are close to the concentrations measured in the street canyon. On the highway, the concentrations in the driving measurements are notably higher than in the stationary measurements. This result was expected as the highway stationary measurement location was approximately 20 m away from the road. Thus, due to the open environment, the emissions from the highway traffic have diluted considerably before getting measured in the highway stationary location. This result agrees with previous studies which have observed that the particle concentrations drop rapidly as the distance from the road increases (Zhu et al., 2002; Massoli et al., 2012). In the city centre, highway and urban road areas, the correlations between BC and LDSA are strong, and the linear fit slopes correspond to the ones measured in the road traffic environments in the stationary measurements. In the harbour area, the slope is again notably higher, which agrees with the stationary measurement results. Thus, it can be considered that the stationary measurement locations are representative of the environments they were categorized to represent, especially in the street canyon and the harbour. In the highway stationary measurements, the concentrations are clearly lower than inside the traffic, but this can be explained with the open environment. More detailed results from the driving measurements are provided in Supplementary (Figs. S19–S23).

Table 3
Averaged BC and LDSA concentrations and the correlation between BC and LDSA in the driving measurement environments.

	City centre	Highway	Urban road	Harbour
BC (μg/m3)	*1.67*	*1.61*	*1.03*	*1.12*
LDSA (μm2/cm3)	*30.0*	*28.9*	*21.3*	*29.6*
BC vs LDSA corr.	$y = 7.17x + 13.86$ $R^2 = 0.97$	$y = 8.12x + 13.27$ $R^2 = 0.93$	$8.58x + 10.32$ $R^2 = 0.97$	$y = 11.53x + 9.02$ $R^2 = 0.92$
Number of data points (30 s)	*663*	*447*	*348*	*181*

3.5. Fraction of the LDSA concentration linked to BC emissions

To analyse the fraction of the total LDSA linked to the BC emissions in the studied environments, the incidence of the measured LDSA per BC concentration -ratios were investigated. This was done to determine the most probable scenario in each studied environment. The probability distributions of the LDSA per BC ratios are shown in Fig. 7. Furthermore, this analysis was done also for the measured LDSA per PM_1 -ratios, which is shown in Supplementary (Fig. S8).

As can be seen, the most probable LDSA per BC -ratios are close to the linear fit slopes shown in Fig. 3. In the road traffic environments, the probability distributions are one-modal and the average ratio between the BC and LDSA concentrations is notably lower than in the harbour. In the harbour, there are clearly two peaks in the probability distribution, which agrees with the results in Fig. 3. The peak with the larger ratios cannot be seen in the road traffic environments, which emphasizes the effects of marine traffic in the harbour area. This similar analysis was done with the measured LDSA and PM_1 concentrations: The most probable LDSA per PM_1 -ratios were 2.92 (2.64–3.93), 2.90 (2.60–3.75) and 2.20 (2.09–2.71) in street canyon, highway and harbour, respectively. Thus, in all the studied environments, BC concentration increase of 1 μg/m^3 is linked to significantly higher LDSA concentration than an equal increase in PM_1, which emphasizes the role of BC emissions in the LDSA concentration in urban environments.

Now, to analyse the average fraction of the LDSA concentration linked to the BC concentration, the measured BC concentrations are multiplied with the factors shown in Fig. 7 and then compared to the measured LDSA concentration. According to this calculation, the fraction of LDSA concentration linked to BC emissions in street canyon, highway and harbour were 33.4 (22.2–50.2) %, 29.8 (19.0–46.8) % and 47.0 (29.7–73.7) %, respectively. In comparison, the fractions of BC mass concentration in PM_1 concentration were 14.1%, 14.4% and 7.1%, respectively. Thus, in all the studied environments, BC emissions contribute much more to LDSA than to mass concentration. This result

indicates that the possible stronger health effects linked with the ambient BC can be related to the high concurrent LDSA concentration. The harbour area results show that the ambient BC can be linked to very high LDSA concentration even though the measured BC mass concentrations are low. The differences between the road traffic and harbour area results show that the lung deposition of ambient BC varies notably in different environments due to the differences in primary emission, aerosol aging processes and co-emitted species, suggesting different toxicity of ambient BC. It needs to be noted that, especially in the harbour, the deviation in the results is very high, which is due to the differences between the road and marine traffic emissions, which both took place in the harbour. Therefore, the relationship between BC and LDSA at a certain location depend on the environmental conditions, e.g. wind direction, in addition to the local emission sources.

The ratio between BC and LDSA depends notably on the other co-emitted compounds than BC. Especially in the harbour, this high LDSA per BC -ratio is affected by the atmospheric condensation processes and coagulation as discussed before. Therefore, the actual role of primary BC in the LDSA concentration in harbour is likely less significant than the calculated 47.0%. Thus, hypothetically it is possible that the other co-emitted compounds than BC could cause high LDSA concentration in harbours even without the simultaneous BC emission. However, the results in Figs. 3, 4 and 6 show that the LDSA and the effects of the other co-emitted compounds are strongly linked to the BC concentration. Thus, black carbon is indeed in a major role in the total LDSA concentration as it can transport the other co-emitted compounds into human lungs effectively. Therefore, the reduction of BC emissions from traffic, where particle filters are not yet adopted, would likely reduce the LDSA concentration caused by the other co-emitted compounds as well.

The results of this study suggest that the harmfulness of equal BC (or PM_1) mass concentration may be notably different in harbour areas than in road traffic environments. The differences in the LDSA size distributions show that the sizes of the lung depositing particles are notably larger in the harbour than in the road traffic sites. Also, the differences in the absorption Ångström exponents indicate that the chemical composition of the lung depositing particles vary between the studied environments. These differences cannot be observed by measuring only the mass concentration of particles, emphasizing the need for other metrics (e.g. LDSA) in the analyses of health effects caused by fine particles. Especially, there is a need for more comprehensive LDSA and BC concentration monitoring in various environments to understand the reasons behind the negative health effects linked to ambient BC more comprehensively.

4. Conclusions

In this study, concentrations of LDSA and ambient BC were investigated in road traffic environments (a street canyon and a highway) and in a harbour. It was found that the characteristics of the lung depositing particles vary notably between these environments. In the street canyon and the highway, the LDSA size distributions peaked near the size of 100 nm, which was expected based on the previous studies. However, in the harbour, the mean size of the LDSA size distributions varied in the size range from 200 nm to 400 nm, which shows that the marine traffic emissions cause LDSA concentrations in notably larger particle sizes than the road traffic. Also, the absorption Ångström exponent of the marine traffic emissions was higher than with the road traffic emissions, which suggests different chemical composition of the lung depositing particles. These observations indicate that the health effects relating the fine particle concentrations differ significantly in harbour areas in comparison with road traffic environments, which should be considered in epidemiological studies relating the fine particle exposure in different urban environments.

It was found that ambient BC has a strong correlation with LDSA concentration in all studied environments. In the road traffic environments, the correlation between BC and LDSA was mainly linear, whereas in the harbour area, the relationship between BC and LDSA was dependent on the value of the absorption Ångström exponent of the measured aerosol, i.e. the dominant emission source. In cases where marine traffic was considered as the main emission source, the average LDSA concentration per BC mass was 2.4–2.7 times higher than in the road traffic environments which suggests that equal BC mass from marine traffic emissions can cause higher exposure of toxic co-emitted compounds in the human lungs than the emissions from road traffic. It was observed that the fractions of LDSA concentration linked to BC emissions in the street canyon, the highway and the harbour were 33.4%, 29.8% and 47.0%, respectively, whereas the fractions of BC mass concentration in PM_1 concentration were 14.1%, 14.4% and 7.1%, respectively. This result shows that BC emissions contribute much more to LDSA than to mass concentration. Thus, it is possible that the more severe health effects of ambient BC compared to the $PM_{2.5}$ are related to the condensation and coagulation of toxic co-emitted compounds and to the high LDSA concentration. The results of this study show that black carbon is indeed in a major role in the total LDSA concentration as it can transport the other co-emitted compounds into human lungs effectively. Thus, the reduction of BC emissions from traffic would reduce the LDSA caused by the other co-emitted compounds as well. Also, it was observed that the characteristics of the lung-depositing BC particles are different in harbour and road traffic environments, which indicate different health effects of ambient BC in these environments.

The results of our study indicate that the BC mass concentration might not be the most ideal metric for the analyses of health effects caused by ambient BC as the LDSA concentration linked to the BC mass concentration is not constant in different environments. This study included road traffic and harbour environments, but it is likely that the connection between BC and LDSA differs also in other environments e.g. residential areas, where characteristics of BC emissions differ notably from the road traffic environments. Therefore, there is a need of both BC and LDSA monitoring measurements and epidemiological studies in various environments and different cities to better understand the health effects relating the lung deposition of ambient BC. Also, more frequent measurements of the LDSA size distribution are needed as it gives more detailed information of the characteristics of the lung depositing particles, which could also explain the different health effects relating the particle exposure in different environments. It needs to be noted that the measured LDSA size distributions in this study indicate that the common diffusion charger based LDSA sensors might underestimate the LDSA concentration in certain environments e.g. harbour, since sensors do not properly detect larger (>300–400 nm) particles. Therefore, measurements of the LDSA size distribution can give valuable information regarding the performance of diffusion charger based LDSA sensors in different environments.

CRediT authorship contribution statement

Teemu Lepistö: Conceptualization, Data curation, Formal analysis, Investigation, Methodology, Visualization, Writing – original draft, Writing – review & editing. **Heino Kuuluvainen:** Conceptualization, Supervision, Investigation, Writing – original draft, Writing – review & editing. **Henna Lintusaari:** Investigation, Methodology, Writing – review & editing. **Niina Kuittinen:** Investigation, Writing – original draft, Writing – review & editing, Project administration. **Laura Salo:** Investigation, Writing – review & editing. **Aku Helin:** Formal analysis, Writing – original draft. **Jarkko V. Niemi:** Resources, Methodology, Writing – review & editing. **Hanna E. Manninen:** Resources, Writing – review & editing. **Hilkka Timonen:** Resources, Writing – original draft, Writing – review & editing, Project administration, Funding acquisition. **Pasi Jalava:** Supervision, Writing – review & editing, Project administration, Funding acquisition. **Sanna Saarikoski:** Resources, Writing – original draft, Writing – review & editing, Project administration, Funding acquisition. **Topi Rönkkö:** Conceptualization, Methodology, Supervision, Writing – original draft, Writing – review & editing, Project

administration, Funding acquisition.

Declaration of competing interest

The authors declare that they have no known competing financial interests or personal relationships that could have appeared to influence the work reported in this paper.

Acknowledgements

This work is part of BC Footprint project (530/31/2019) funded by Business Finland and participating companies.

This work has received funding from the European Union's Horizon 2020 research and innovation programme under grant agreement No 814978 (TUBE: Transport-derived ultrafines and the brain effects).

We gratefully acknowledge Academy of Finland Flagship funding Atmosphere and Climate Competence Center, ACCC (grant no. 337552, 337551).

We wish to thank Lassi Markkula, Leonardo De Oliveira Negri, Janne Huhtala, Elmeri Laakkonen and Katja Mustonen as well as HSY's measurement team for their valuable work during the measurement campaign.

Appendix A. Supplementary data

Supplementary data to this article can be found online at https://doi.org/10.1016/j.atmosenv.2021.118931.

References

Aguilera, I., Dratva, J., Caviezel, S., Burdet, L., de Groot, E., Ducret-Stich, R.E., Eeftens, M., Keidel, D., Meier, R., Perez, L., Rothe, T., Schaffner, E., Schmit-Trucksäss, A., Tsai, M.Y., Schindler, C., Künzli, N., Probst-Hensch, N., 2016. Particulate matter and subclinical atherosclerosis: associations between different particle sizes and sources with carotid intimamedia thickness in the SAPALDIA study. Environ. Health Perspect. 124, 1700–1706. https://doi.org/10.1289/EHP161.

Amanatidis, S., Ntziachristos, L., Karjalainen, P., Saukko, E., Simonen, P., Kuittinen, N., Aakko-Saksa, P., Timonen, H., Rönkkö, T., Keskinen, J., 2018. Comparative performance of a thermal denuder and a catalytic stripper in sampling laboratory and marine exhaust aerosols. Aerosol. Sci. Technol. 52 (4), 420–432. https://doi.org/10.1080/02786826.2017.1422236.

Barreira, L.M.F., Helin, A., Aurela, M., Teinilä, K., Friman, M., Kangas, L., Niemi, J.V., Portin, H., Kousa, A., Pirjola, L., Rönkkö, T., Saarikoski, S., Timonen, H., 2021. In-depth characterization of submicron particulate matter inter-annual variations at a street canyon site in northern Europe. Atmos. Chem. Phys. 21, 6297–6314. https://doi.org/10.5194/acp-21-6297-2021.

Becerril-Valle, M., Coz, E., Prévôt, A.S.H., Močnik, G., Pandis, S.N., Sánchez de la Campa, A.M., Alastuey, A., Díaz, E., Pérez, R.M., Artíñano, B., 2017. Characterization of atmospheric black carbon and co-pollutants in urban and rural areas of Spain. Atmos. Environ. 169, 36–53. https://doi.org/10.1016/j.atmosenv.2017.09.014.

Bond, T.C., et al., 2013. Bounding the role of black carbon in the climate system: a scientific assessment. J. Geophys. Res. Atmos. 118, 5380–5552. https://doi.org/10.1002/jgrd.50171.

Brown, D.M., Wilson, M.R., MacNee, W., Stone, V., Donaldson, K., 2001. Size-dependent proinflammatory effects of ultrafine polystyrene particles: a role for surface area and oxidative stress in the enhanced activity of ultrafines. Toxicol. Appl. Pharmacol. 175 (3), 191–199. https://doi.org/10.1006/taap.2001.9240.

Burnett, R.T., Pope, C.I.I., Ezzati, M., Olives, C., Lim, S.S., Mehta, S., Shin, H.H., Singh, G., Hubbell, B., Brauer, M., et al., 2014. An integrated risk function for estimating the global burden of disease attributable to ambient fine particulate matter exposure. Environ. Health Perspect. 122 (4), 397–403. https://doi.org/10.1289/ehp.1307049.

Cesari, D., Genga, A., Ielpo, P., Siciliano, M., Mascolo, G., Grasso, F.M., Contini, D., 2014. Source apportionment of PM2.5 in the harbour–industrial area of Brindisi (Italy): identification and estimation of the contribution of in-port ship emissions. Sci. Total Environ. 497-498, 392. https://doi.org/10.1016/j.scitotenv.2014.08.007, 400.

Cheristanidis, S., Grivas, G., Chaloulakou, A., 2020. Determination of total and lung-deposited particle surface area concentrations, in central Athens, Greece. Environ. Monit. Assess. 192, 627. https://doi.org/10.1007/s10661-020-08569-8.

Ching, J., Kajino, M., Matsui, H., 2020. Resolving aerosol mixing state increases accuracy of black carbon respiratory deposition estimates, 2020 One Earth 3 (6), 763–776. https://doi.org/10.1016/j.oneear.2020.11.004. ISSN 2590-3322.

Cohen, A.J., Brauer, M., Burnett, R., Anderson, H.R., Frostad, J., Estep, K., Balakrishnan, K., Brunekreef, B., Dandona, L., Dandona, R., et al., 2017. Estimates and 25-year trends of the global burden of disease attributable to ambient air pollution: an analysis of data from the Global Burden of Diseases Study 2015. Lancet 389 (10082), 1907–1918. https://doi.org/10.1016/S0140-6736(17)30505-6.

Corbin, J.C., Pieber, S.M., Czech, H., Zanatta, M., Jakobi, G., Massabò, D., et al., 2018. Brown and black carbon emitted by a marine engine operated on heavy fuel oil and distillate fuels: optical properties, size distributions, and emission factors. J. Geophys. Res. Atmos. 123, 6175–6195. https://doi.org/10.1029/2017JD027818.

Dockery, D.W., Pope, C.A., Xu, X., Spengler, J.D., Ware, J.H., Fay, M.E., Ferris Jr., B.G., Speizer, F.E., 1993. An association between air pollution and mortality in six U.S. cities. N. Engl. J. Med. 329 (24), 1753–1759. https://doi.org/10.1056/NEJM199312093292401.

Drinovec, L., Mocnik, G., Zotter, P., Prévôt, A.S.H., Ruckstuhl, C., Coz, E., Rupakheti, M., Sciare, J., Müller, T., Wiedensohler, A., Hansen, A.D.A., 2015. The "dual-spot" Aethalometer: an improved measurement of aerosol black carbon with real-time loading compensation. Atmos. Meas. Tech. 8, 1965–1979. https://doi.org/10.5194/amt-8-1965-2015.

Gemmer, M., Xiao, B., 2013. Air quality legislation and standards in the European union: background, status and public participation. Adv. Clim. Change Res. 4 (1), 50–59. https://doi.org/10.3724/SP.J.1248.2013.050.

Gentner, D.R., Jathar, S.H., Gordon, T.D., Bahreini, R., Day, D.A., El Haddad, I., Hayes, P. L., Pieber, S.M., Platt, S.M., Gouw, J. de, Goldstein, A.H., Harley, R.A., Jimenez, J.L., Prévôt, A.S.H., Robinson, A.L., 2017. Review of urban secondary organic aerosol formation from gasoline and diesel motor vehicle emissions. Environ. Sci. Technol. 51 (3), 1074–1093. https://doi.org/10.1021/acs.est.6b04509.

Hama, S.M.L., Ma, N., Cordell, R.L., Kos, G.P.A., Wiedensohler, A., Monks, P.S., 2017. Lung deposited surface area in Leicester urban background site/UK: sources and contribution of new particle formation. Atmos. Environ. 151, 94–107. https://doi.org/10.1016/j.atmosenv.2016.12.002.

Happonen, M., Mylläri, F., Karjalainen, P., Frey, A., Saarikoski, S., Carbone, S., Hillamo, R., Pirjola, L., Häyrinen, A., Kytömäki, J., Niemi, J.V., Keskinen, J., Rönkkö, T., 2013. Size distribution, chemical composition, and hygroscopicity of fine particles emitted from an oil-fired heating plant. Environ. Sci. Technol. 47 (24), 14468–14475. https://doi.org/10.1021/es4028056.

Heikkilä, J., Virtanen, A., Rönkkö, T., Keskinen, J., Aakko-Saksa, P., Murtonen, T., 2009. Environ. Sci. Technol. 43 (24), 9501–9506. https://doi.org/10.1021/es9013807.

Helin, A., Niemi, J.V., Virkkula, A., Pirjola, L., Teinilä, K., Backman, J., Aurela, M., Saarikoski, S., Rönkkö, T., Asmi, E., Timonen, H., 2018. Characteristics and source apportionment of black carbon in the Helsinki metropolitan area, Finland. Atmos. Environ. 190, 87–98. https://doi.org/10.1016/j.atmosenv.2018.07.022.

Helin, A., Virkkula, A., Backman, J., Pirjola, L., Sippula, O., Aakko-Saksa, P., Väätäinen, S., Mylläri, F., Järvinen, A., Bloss, M., Aurela, M., Jakobi, G., Karjalainen, P., Zimmermann, R., Jokiniemi, J., Saarikoski, S., Tissari, J., Rönkkö, T., Niemi, J.V., Timonen, H., 2021. Variation of absorption Ångström exponent in aerosols from different emission sources. Geophys. Res. Atmos. 126 https://doi.org/10.1029/2020JD034094.

Hennig, F., Quass, U., Hellack, B., Küpper, M., Kuhlbusch, T.A.J., Stafoggia, Massimo, Hoffmann, Barbara, 2018. Ultrafine and fine particle number and surface area concentrations and daily cause-specific mortality in the Ruhr area, Germany, 2009–2014. Environ. Health Perspect. 126 https://doi.org/10.1289/EHP2054.

Henning, S., Ziese, M., Kiselev, A., Saathoff, H., Möhler, O., Mentel, T.F., Buchholz, A., Spindler, C., Michaud, V., Monier, M., Sellegri, K., Stratmann, F., 2012. Hygroscopic growth and droplet activation of soot particles: uncoated, succinic or sulfuric acid coated. Atmos. Chem. Phys. 12, 4525–4537. https://doi.org/10.5194/acp-12-4525-2012.

Heusinkveld, H., Wahle, T., Campbell, A., Westerink, R., Tran, L., Johnston, H., Stone, V. R., Cassee, F., Schins, R., 2016. Neurodegenerative and neurological disorders by small inhaled particles. Neurotoxicology 113, 94–106. https://doi.org/10.1016/j.neuro.2016.07.007.

ICRP, 1994. Human Respiratory Tract Model for Radiological Protection, vol. 66, p. 24.

Janssen, N., Hoek, G., Simic-Lawson, M., Fischer, P., Bree, L. van, Brink, H. ten, Keuken, M., Atkinson, R.W., Anderson, H.R., Brunekreef, B., Cassee, F.R., 2011. Black carbon as an additional indicator of the adverse health effects of airborne particles compared with PM10 and PM2.5. Environ. Health Perspect. 119, 12. https://doi.org/10.1289/ehp.1003369.

Jeong, C.H., Traub, A., Evans, G.J., 2017. Exposure to ultrafine particles and black carbon in diesel-powered commuter trains. Atmos. Environ. 155 (46–52), 1352–2310. https://doi.org/10.1016/j.atmosenv.2017.02.015.

Järvinen, A., Aitomaa, M., Rostedt, A., Keskinen, J., Yli-Ojanperä, J., 2014. Calibration of the new electrical low pressure impactor (ELPI+). J. Aerosol Sci. 69, 150–159. https://doi.org/10.1016/j.jaero-sci.2013.12.006.

Karttunen, S., Kurppa, M., Auvinen, M., Hellsten, A., Järvi, L., 2020. Large-eddy Simulation of the Optimal Street-Tree Layout for Pedestrian-Level Aerosol Particle Concentrations – A Case Study from a City-Boulevard, vol. X. Atmospheric Environment, p. 6. https://doi.org/10.1016/j.aeaoa.2020.100073.

Keskinen, J., Pietarinen, K., Lehtimäki, M., 1992. Electrical low pressure impactor. J. Aerosol Sci. 23 (4), 353–360. https://doi.org/10.1016/0021-8502(92)90004-F.

Kirchstetter, T., Novakov, T., Hobbs, P., 2004. Evidence that the spectral dependence of light absorption by aerosols is affected by organic carbon. J. Geophys. Res. Atmos. 109, 21. https://doi.org/10.1029/2004JD004999.

Krasowsky, T.S., McMeeking, G.R., Wang, D., Sioutas, C., Ban-Weiss, G.A., 2016. Measurements of the impact of atmospheric aging on physical and optical properties of ambient black carbon particles in Los Angeles. Atmos. Environ. 142, 496–504. https://doi.org/10.1016/j.atmosenv.2016.08.010.

Kumar, P., Robins, A., Vardoulakis, S., Britter, S., 2010. A review of the characteristics of nanoparticles in the urban atmosphere and the prospects for developing regulatory controls. Atmos. Environ. 44 (39), 5035–5052. https://doi.org/10.1016/j.atmosenv.2010.08.016.

Kuula, J., Kuuluvainen, H., Niemi, J.V., Saukko, E., Portin, H., Kousa, A., Aurela, M., Rönkkö, T., Timonen, H., 2020. Long-term sensor measurements of lung deposited surface area of particulate matter emitted from local vehicular and residential wood combustion sources. Aerosol. Sci. Technol. 54 (2), 190–202. https://doi.org/10.1080/02786826.2019.1668909.

Kuuluvainen, H., Rönkkö, T., Järvinen, A., Saari, S., Karjalainen, P., Lähde, T., Pirjola, L., Niemi, J.V., Hillamo, R., Keskinen, J., 2016. Lung deposited surface area size distributions of particulate matter in different urban areas. Atmos. Environ. 136, 105–113. https://doi.org/10.1016/j.atmosenv.2016.04.019.

Lack, D.A., Cappa, C.D., 2010. Impact of brown and clear carbon on light absorption enhancement, single scatter albedo and absorption wavelength dependence of black carbon. Atmos. Chem. Phys. 10, 4207–4220. https://doi.org/10.5194/acp-10-4207-2010.

Lelieveld, J., Evans, J., Fnais, M., et al., 2015. The contribution of outdoor air pollution sources to premature mortality on a global scale. Nature 525, 367–371. https://doi.org/10.1038/nature15371.

Lepistö, T., Kuuluvainen, H., Juuti, P., Järvinen, A., Arffman, A., Rönkkö, T., 2020. Measurement of the human respiratory tract deposited surface area of particles with an electrical low pressure impactor. Aerosol. Sci. Technol. https://doi.org/10.1080/02786826.2020.1745141.

Li, X., Jin, L., Kan, H., 2019. Air pollution: a global problem needs local fixes. Nature 570 (7762), 437–439. https://doi.org/10.1038/d41586-019-01960-7.

Lin, T.-C., Chiueh, P.-T., Griffith, S.M., Liao, C.-C., Hsiao, T.-C., 2022. Deployment of a Mobile Platform to Characterize Spatial and Temporal Variation of On-Road Fine Particles in an Urban Area, vol. 204. Environmental Research. https://doi.org/10.1016/j.envres.2021.112349.

Luoma, K., Niemi, J.V., Aurela, M., Fung, P.L., Helin, A., Hussein, T., Kangas, L., Kousa, A., Rönkkö, T., Timonen, H., Virkkula, A., Petäjä, T., 2021. Spatiotemporal variation and trends in equivalent black carbon in the Helsinki metropolitan area in Finland. Atmos. Chem. Phys. 21, 1173–1189. https://doi.org/10.5194/acp-21-1173-2021.

Marjamäki, M., Keskinen, J., Chen, D., Pui, D.Y.H., 2000. Performance evaluation of the electrical low pressure impactor (ELPI). J. Aerosol Sci. 31 (2), 249–261. https://doi.org/10.1016/S0021-8502(99)00052-X.

Massoli, P., Fortner, E.C., Canagaratna, M.R., Williams, L.R., Zhang, Q., Sun, Y., Schwab, J.J., Trimborn, A., Onasch, T.B., Demerjian, K.L., Kolb, C.E., Worsnop, D.R., Jayne, J.T., 2012. Pollution gradients and chemical characterization of particulate matter from vehicular traffic near major roadways: results from the 2009 queens college air quality study in NYC. Aerosol. Sci. Technol. 46 (11), 1201–1218. https://doi.org/10.1080/02786826.2012.701784.

Ntziachristos, L., Polidori, A., Phuleria, H., Geller, M.D., Sioutas, C., 2007. Application of a diffusion charger for the measurement of particle surface concentration in different environments. Aerosol Sci. Technol. 41, 571–580. https://doi.org/10.1080/02786820701272020.

Ntziachristos, L., Saukko, E., Lehtoranta, K., Rönkkö, T., Timonen, H., a, P.S., Karjalainen, P., Keskinen, J., 2016. Particle emissions characterization from a medium-speed marine diesel engine with two fuels at different sampling conditions. Fuel 186, 456–465. https://doi.org/10.1016/j.fuel.2016.08.091.

Oberdorster, G., Oberdorster, E., Oberdorster, J., 2005. Nanotoxicology: an emerging discipline evolving from studies of ultrafine particles. Environ. Health Perspect. 113 (7), 823–839. https://doi.org/10.1289/ehp.7339.

Patel, S., Leavey, A., Sheshadri, A., et al., 2018. Associations between household air pollution and reduced lung function in women and children in rural southern India. J. Appl. Toxicol. 38, 1405–1415. https://doi.org/10.1002/jat.3659.

Pirjola, L., Niemi, J.V., Saarikoski, S., Aurela, M., Enroth, J., Carbone, S., Saarnio, K., Kuuluvainen, H., Kousa, A., Rönkkö, T., Hillamo, R., 2017. Physical and chemical characterization of urban winter-time aerosols by mobile measurements in Helsinki, Finland. Atmos. Environ. 158, 60–75. https://doi.org/10.1016/j.atmosenv.2017.03.028.

Pope III, C.A., Burnett, R.T., Thun, M.J., et al., 2002. Lung cancer, cardiopulmonary mortality, and long-term exposure to fine particulate air pollution. JAMA 287 (9), 1132–1141. https://doi.org/10.1001/jama.287.9.1132.

Power, M.C., Adar, S.D., Yanosky, J.D., Weuve, J., 2016. Exposure to air pollution as a potential contributor to cognitive function, cognitive decline, brain imaging, and dementia: a systematic review of epidemiologic research. Neurotoxicology 56, 235–253. https://doi.org/10.1016/j.neuro.2016.06.004.

Reche, C., Viana, M., Brines, M., Pérez, N., Beddows, D., Alastuey, A., Querol, X., 2015. Determinants of aerosol lung-deposited surface area variation in an urban environment. Sci. Total Environ. 517, 38–47. https://doi.org/10.1016/j.scitotenv.2015.02.049.

Raaschou-Nielsen, O., Andersen, Z.J., Beelen, R., Samoli, E., Stafoggia, M., Weinmayr, G., Hoffmann, B., Fischer, P., Nieuwenhuijsen, M.J., Brunekreef, B., et al., 2013. Air pollution and lung cancer incidence in 17 European cohorts: prospective analyses from the European study of cohorts for air pollution effects (ESCAPE). Lancet Oncol. 14, 813–822. https://doi.org/10.1016/S1470-2045(13)70279-1.

Rissler, J., Nordin, E.Z., Eriksson, A.C., Nilsson, P.T., Frosch, M., Sporre, M.K., Wierzbicka, A., Svenningsson, B., Löndahl, J., Messing, M.E., et al., 2014. Effective density and mixing state of aerosol particles in a near-traffic urban environment. Environ. Sci. Technol. 48 (11), 6300–6308. https://doi.org/10.1021/es5000353.

Salo, L., Hyvärinen, A., Jalava, P., Teinilä, K., Hooda, R.K., Datta, A., Saarikoski, S., Lintusaari, H., Lepistö, T., Martikainen, S., et al., 2021. The characteristics and size of lung-depositing particles vary significantly between high and low pollution traffic environments. Atmos. Environ. 255, 118421. https://doi.org/10.1016/j.atmosenv.2021.118421.

Sandradewi, J., Prévôt, A.S.H., Szidat, S., Perron, N., Rami Alfarra, M., Lanz, V.A., Weingartner, E., Baltensperger, U., 2008. Using aerosol light absorption measurements for the quantitative determination of wood burning and traffic emission contributions to particulate matter. Environ. Sci. Technol. 42, 3316–3323. https://doi.org/10.1021/es702253m.

Schmid, O., Stoeger, T., 2016. Surface area is the biologically most effective dose metric for acute nanoparticle toxicity in the lung. J. Aerosol Sci. 99, 133–143. https://doi.org/10.1016/j.jaerosci.2015.12.006.

Singh, V., Ravindra, K., Sahu, L., Sokhi, R., 2018. Trends of atmospheric black carbon concentration over the United Kingdom. Atmos. Environ. 178, 148–157. https://doi.org/10.1016/j.atmosenv.2018.01.030.

Todea, A.M., Beckmann, S., Kaminski, H., Asbach, C., 2015. Accuracy of electrical aerosol sensors measuring lung deposited surface are concentrations. J. Aerosol Sci. 89, 96–109. https://doi.org/10.1016/j.jaerosci.2015.07.003.

Viana, M., Hammingh, P., Colette, A., Querol, X., Degraeuwe, B., Vlieger, I. de, Aardenne, J., 2014. Impact of maritime transport emissions on coastal air quality in Europe. Atmos. Environ. 90, 96–105. https://doi.org/10.1016/j.atmosenv.2014.03.046.

Virkkula, A., 2021. Modeled source apportionment of black carbon particles coated with a light-scattering shell. Atmos. Meas. Tech. 14, 3707–3719. https://doi.org/10.5194/amt-14-3707-2021.

Vohra, K., Vodonos, A., Schwartz, J., Marais, E.A., Sulprizio, M.P., Mickley, L.J., 2021. Global mortality from outdoor fine particle pollution generated by fossil fuel combustion: results from. GEOS-Chem. Environ. Res. 195, 110754. https://doi.org/10.1016/j.envres.2021.110754. ISSN 0013-9351.

Xiao, Q., Li, M., Liu, H., Fu, M., Deng, F., Lv, Z., Man, H., Jin, X., Liu, S., He, K., 2018. Characteristics of marine shipping emissions at berth: profiles for particulate matter and volatile organic compounds. Atmos. Chem. Phys. 18, 9527–9545. https://doi.org/10.5194/acp-18-9527-2018.

Yu, G.-H., Park, S., Shin, S.-K., Lee, K.-H., Nam, H.-G., 2018. Enhanced light absorption due to aerosol particles in ship plumes observed at a seashore site. Atmos. Pollut. Res. 9 (6), 1177–1183. https://doi.org/10.1016/j.apr.2018.05.005.

Zhu, Y., Hinds, W.C., Kim, S., Sioutas, C., 2002. Concentration and size distribution of ultrafine particles near a major highway. J. Air Waste Manag. Assoc. 52 (9), 1032–1042. https://doi.org/10.1080/10473289.2002.10470842.

Zotter, P., Herich, H., Gysel, M., El-Haddad, I., Zhang, Y., Močnik, G., Hüglin, C., Baltensperger, U., Szidat, S., Prévôt, A.S.H., 2017. Evaluation of the absorption Ångström exponents for traffic and wood burning in the Aethalometer-based source apportionment using radiocarbon measurements of ambient aerosol. Atmos. Chem. Phys. 17, 4229–4249. https://doi.org/10.5194/acp-17-4229-2017.